Phase Diagram of a Geometrically Frustrated Triangular-Lattice Antiferromagnet in a Magnetic Field

Randy S. Fishman

Materials Science and Technology Division, Oak Ridge National Laboratory, Oak Ridge, Tennessee 37831, USA

(Received 30 September 2010; revised manuscript received 3 January 2011; published 20 January 2011)

The magnetic phase diagram of a geometrically frustrated triangular-lattice antiferromagnet is evaluated as a function of magnetic field and anisotropy using a trial spin state built from harmonics of a fundamental ordering wave vector. A noncollinear incommensurate state, observed to be chiral and ferroelectric in $CuFeO_2$, appears above a collinear state with 4 sublattices (SLs). The apparent absence of multiferroic behavior for predicted chiral, noncollinear 5-SL states poses a challenge to theories of the ferroelectric coupling in $CuFeO_2$.

DOI: 10.1103/PhysRevLett.106.037206 PACS numbers: 75.10.Hk, 75.30.Kz, 75.50.Ee

Several multiferroic materials with noncollinear (NC) spin states exhibit strong coupling between their magnetic and ferroelectric moments. Two possible mechanisms have been proposed to explain the magnetoelectric coupling in these "improper" mutliferroics [1]. An electric polarization $\mathbf{P}$ perpendicular to both the spin chirality $\mathbf{C}$ and the wave vector $\mathbf{Q}$ is predicted for ferroelectrics like $R\mathrm{MnO_3}$ (R = Tb or Y), which have easy-plane anisotropy and spiral spin states that break inversion symmetry [2]. Because $\mathbf{C}$ is parallel to $\mathbf{Q}$ in easy-axis compounds like $CuFeO_2$ [3] and $CuCrO_2$ [4], their multiferroic behavior has been explained by the modulation of the metal-ligand hybridization with the spin-orbit coupling [5,6], which predicts that $\mathbf{P}$ is parallel to both $\mathbf{Q}$ and $\mathbf{C}$. Since different coupling mechanisms apply to different types of spin structures, it is important to understand how the chiral and noncollinear spin structures of multiferroic materials evolve with doping and magnetic field.

Particularly intriguing is the NC and incommensurate ferroelectric phase observed in $CuFeO_2$ for fields between 7 and 13.5 T [7–9]. Below 7 T, the magnetic ground state is the collinear (CL), 4-sublattice (SL) state (CL-4 state) in Fig. 1(b); above 13.5 T, the ground state is believed to be the CL-5i state in Fig. 1(c). This Letter constructs the magnetic phase diagram of a geometrically frustrated triangular-lattice antiferromagnet (TLA), which accurately predicts [10] the spin states of doped $CuFeO_2$ in zero field. In addition to the expected CL and NC states, we find that the NC 5-SL states (NC-5 states) sketched in Fig. 1(e) appear for fields above and below the CL-5i phase and between the CL-3 phase in Fig. 1(a) and a spin-flop (SF) phase.

The energy of a geometrically frustrated TLA in a magnetic field H along the $\mathbf{z}$ direction can be written

$$E = -\frac{1}{2}\sum_{i\neq j} J_{ij}\mathbf{S}_i\cdot\mathbf{S}_j - D\sum_i {S_{iz}}^2 - 2\mu_B H\sum_i S_{iz}, \quad (1)$$

where $\mathbf{S}_i \equiv \mathbf{S}(\mathbf{R}_i)$ are classical spins. The easy-axis anisotropy D favors the CL states sketched in Fig. 1 with spins aligned along the z axis. Recent results suggest that D can be reduced in $CuFeO_2$ by either Al or Ga doping [11,12] and may be enhanced by deficient ($\delta < 0$) or excess ($\delta > 0$) oxygen [13] in the nonstoichiometric compound $CuFeO_{2+\delta}$. The exchange pathways for the nearest-neighbor interaction $J_1 < 0$ as well as for the second- and third-neighbor interactions J_2 and J_3 are indicated in Fig. 1(a). Because of the large $S = 5/2$ spin of Fe^{3+}, the assumption of classical spins should incur minimal error. Because the antiferromagnetic coupling between neighboring hexagonal layers in $CuFeO_2$ is not frustrated, Eq. (1) should provide qualitatively accurate predictions for the phase diagram of $CuFeO_2$ in a magnetic field.

For $D \gg |J_1|$ and $H = 0$, the phase diagram of Eq. (1) contains CL states with 1, 2, 3, 4, or 8 SLs [14]. Except for the CL-1 or paramagnetic (PM) state with all spins aligned, the other CL states become unstable to NC states with decreasing D [15]. The CL-4 region of the $\{J_2/|J_1|, J_3/|J_1|\}$ phase diagram is given by the conditions $J_3 < J_2/2$ and $-0.5 < J_2/|J_1| < 0$. This region contains

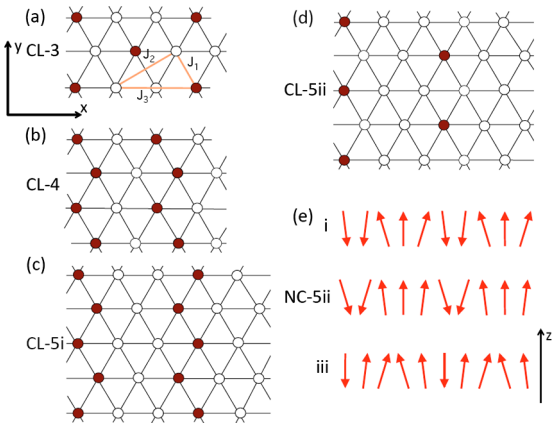

FIG. 1 (color online). CL phases with (a) three, (b) four, or (c), (d) five SLs. White circles have spin-up and dark circles have spin-down. Also shown in (a) are the exchange pathways for the interactions J_1, J_2, and J_3. NC-5 states are sketched in (e).

two subregions: subregion 4II in the lower right where the wave vector $(4\pi/3)\mathbf{x}$ of the NC state is independent of the exchange interactions and subregion 4I in the upper left where the incommensurate wave vector $Q\mathbf{x}$ of the NC state sensitively depends on $J_2/|J_1|$ and $J_3/|J_1|$ [15,16]. Since the wave vector of doped $CuFeO_2$ in its multiferroic phase is approximately $0.85\pi\mathbf{x}$, pure $CuFeO_2$ lies in subregion 4I with exchange interactions $J_2/|J_1| \approx -0.44$ and $J_3/|J_1| \approx -0.57$ [17].

To evaluate the phase diagram as a function of field and anisotropy, we generalize an earlier approach [10] by constructing trial spin states built on harmonics of the fundamental ordering wave vector $Q\mathbf{x}$:

$$S_z(\mathbf{R}) = S_0 + \sum_{l=1}^{\infty} C_l \cos(Qlx), \tag{2}$$

$$S_y(\mathbf{R}) = \sqrt{S^2 - S_z(\mathbf{R})^2}\,\mathrm{sgn}[\sin(Qx)], \tag{3}$$

and $S_x(\mathbf{R}) = 0$. For convenience, the lattice constant is set to 1. Whereas the trial spin state in zero field only included odd harmonics C_{2l+1}, both odd and even harmonics are required in nonzero field [18]. For the results presented below, only terms up to C_5 are significant. Consequently, a trial incommensurate spin state has six variational parameters (Q and $C_{l\le 5}$) with S_0 fixed by the constraint that the maximum value of $S_z(\mathbf{R})$ is $S = 5/2$.

Another trial spin state is introduced for the conical SF phase in high fields: $S_x(\mathbf{R}) = A\cos(Qx)$, $S_y(\mathbf{R}) = A\sin(Qx)$, and $S_z(\mathbf{R}) = \sqrt{S^2 - A^2}$. Because the anisotropy D acts along the z axis, the SF state does not contain anharmonic distortions in the xy plane. Therefore, the trial SF state contains only two variational parameters: Q and A.

For incommensurate states, the energy E was minimized within a unit cell of length 5000 with open boundary conditions in the x direction using the parameters $J_2/|J_1| = -0.44$ and $J_3/|J_1| = -0.57$ believed to describe pure $CuFeO_2$. Of course, E can be minimized in a much smaller unit cell for commensurate states. Numerical results are checked by assuring that each spin $\mathbf{S}_i$ is locally in equilibrium.

The resulting magnetic phase diagram for $D/|J_1| \le 0.6$ is plotted in Fig. 2. Five CL phases appear with 1, 3, 4, or 5 SLs. As shown in Figs. 1(c) and 1(d), the CL-5i or ↑↑↑↓↓ state has a net normalized spin of $M \equiv \langle S_{iz}\rangle/S = 1/5$ while the CL-5ii or ↑↑↑↑↓ state has $M = 3/5$. The CL-3 state has $M = 1/3$ and the CL-4 or ↑↑↓↓ state found in pure $CuFeO_2$ in zero field has no net spin. A CL-1 or PM state has $M = 1$. The energies and net normalized spins of all CL phases are summarized [19] in Table I, which defines $h = 2\mu_B H/S$.

Three distinct NC-5 regions with $\mathbf{Q} = 0.8\pi\mathbf{x}$ were identified. The NC-5 states can be obtained by canting the spins of the CL states in the neighboring CL-5i and CL-5ii regions while retaining the 5-SL periodicity and keeping the spins in the yz plane. Minimizing the energy for these

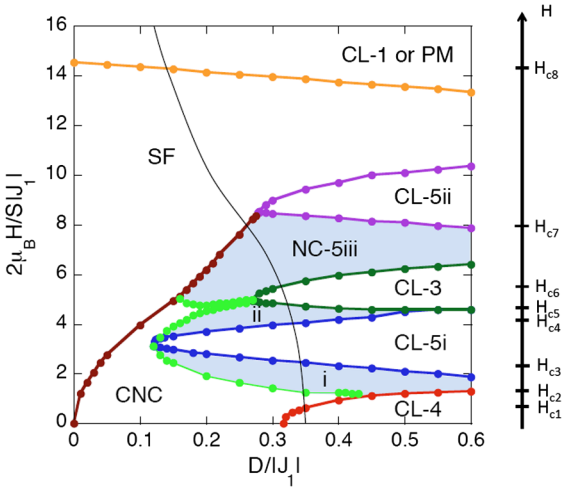

FIG. 2 (color online). The magnetic phase diagram as a function of external field and anisotropy for $J_2/|J_1| = -0.44$ and $J_3/|J_1| = -0.57$. A possible trajectory through this phase diagram for $CuFeO_2$ is given by the thin solid curve with critical fields indicated on the right. NC-5i, NC-5ii, and NC-5iii regions are shaded.

states is simplified by the fact that the higher harmonics $n\mathbf{Q}$ with $n > 2$ can be expressed in terms of $\mathbf{Q}$, $2\mathbf{Q}$, and the reciprocal lattice vector $\mathbf{G} = 4\pi\mathbf{x}$. With increasing field from top to bottom, the NC-5i ($M < 0.2$), NC-5ii ($M > 0.2$), and NC-5iii ($M < 0.6$) states are sketched in Fig. 1(e). The spin configurations and net spins M of the NC-5 states change with field.

A SF phase appears below the PM phase. Since the SF phase remains stable as $H \to 0$ for $D = 0$ ($\mu_B H_c \propto \sqrt{|J_1|D}$ for $D/|J_1| \ll 1$), the SF transition occurs at zero field in the absence of anisotropy. For the parameters in Fig. 2, the incommensurate wave vector of the SF phase is $Q \approx 0.853\pi$ for all D and H.

Complex, NC, and incommensurate states (CNC states) produced by Eqs. (2) and (3) appear outside the CL and NC-5 regions and below the SF transition. CNC states disappear above $D/|J_1| \approx 0.41$, at the juncture between the NC-5i and CL-4 phases. The CNC phase also terminates at the leftmost point of the CL-3 phase with $D/|J_1| \approx 0.27$. Although predominantly determined by the exchange interactions, the wave vector of the CNC phase increases slightly with anisotropy [12] and decreases slightly with field: for $H = 0$, Q increases from 0.853π at $D = 0$ to 0.860π at $D/|J_1| = 0.3$; for $D/|J_1| = 0.1$, Q decreases

TABLE I. Energies and net spins of the CL states.

Phase		E/NS^2	M
CL-1	1(1,0)	$-3(J_1 + J_2 + J_3) - D - h$	1
CL-3	3(2,1)	$J_1 - 3J_2 + J_3 - D - h/3$	1/3
CL-4	4(2,2)	$J_1 - J_2 + J_3 - D$	0
CL-5i	5(3,2)	$(J_1 + J_2)/5 + J_3 - D - h/5$	1/5
CL-5ii	5(4,1)	$-3(J_1 + J_3)/5 - 7J_2/5 - D - 3h/5$	3/5

from 0.857π at $H = 0$ to 0.835π at $2\mu_B H/S|J_1| = 3.95$, which is the CNC → SF phase boundary.

Figure 3 plots the net spin M versus field for $D/|J_1| = 0$, 0.2, 0.4, and 0.6. Notice that M is a linear function of field in both the SF and NC-5 phases. For $D/|J_1| = 0.6$, first-order jumps in M occur at the CL-4 → NC-5i, CL-5i → CL-3 → NC-5iii, and CL-5ii → SF transitions. For smaller $D/|J_1|$, M evolves smoothly within the CNC phase but jumps at the CNC → NC-5i and CNC → SF transitions. Because the NC-5 states can be transformed into the CL-5i and CL-5ii states without altering the 5-SL periodicity, the NC-5i → CL-5i → NC-5ii and NC-5iii → CL-5ii transitions are second order.

The bottom of Fig. 3 plots the amplitude of the chirality $\mathbf{C} = \langle \mathbf{S}(\mathbf{R}) \times \mathbf{S}(\mathbf{R} + \mathbf{x}/2) \rangle / S^2$ versus field. For the CNC and NC-5 phases, $\mathbf{C}$ lies along the x axis; for the SF phase, $\mathbf{C}$ lies along the z axis. Of course, the chirality of the CL states vanishes. The chirality of the SF phase is given by $C = (1 - M^2)\sin(Q/2)$ and vanishes as $M \to 1$. For any field, the CNC and NC-5 phases always have a chirality smaller than that of the $D = 0$ SF phase. Generally, the chirality of the NC-5iii phase is larger than that of the NC-5i and NC-5ii phases. For $D/|J_1| = 0.2$ and 0.4, the chirality of the lowest CNC phase is larger than that of the NC-5i phase.

The first theoretical study of the magnetic phase diagram of $CuFeO_2$ was performed by Ajiro *et al.* [20], who used Ising spins [the $D \to \infty$ limit of Eq. (1)] to obtain the following sequence of transitions: CL-4 → CL-5i → CL-3 → CL-7i → CL-7ii → PM. For $D/|J_1| = 0.6$, either the CL-5ii, NC-5iii, or SF phase has lower energy than the CL-7i [or 7(5,2)] and CL-7ii [or 7(6,1)] phases [19].

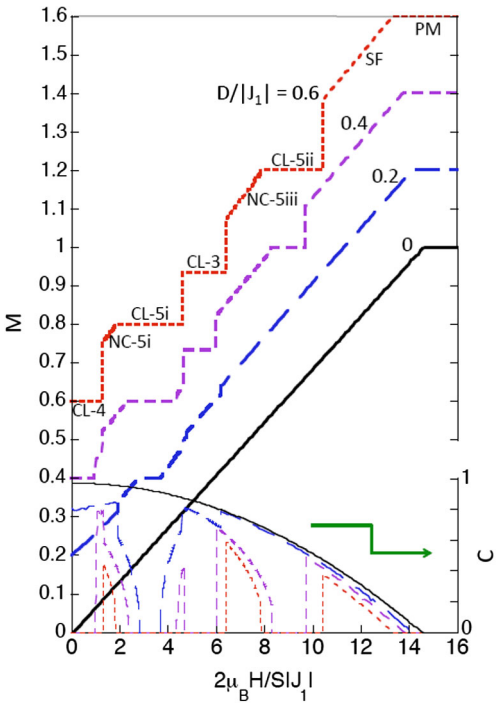

FIG. 3 (color online). The net normalized spin M as a function of field (sequentially offset by $\Delta M = 0.2$) as well as the chirality C of the NC phases in the bottom panel for $D/|J_1| = 0$ (solid line), 0.2 (long dashed line), 0.4 (medium dashed line), and 0.6 (short dashed line). Other parameters as in Fig. 2.

Based on a three-dimensional Hamiltonian that includes both symmetric and antisymmetric biquadratic exchange terms, Plumer [21] obtained a spiral incommensurate phase between the CL-4 and CL-5i phases. Extending that work, Quirion *et al.* [22] predicted another spiral phase between the CL-3 and SF phases. Lummen *et al.* [23] employed a two-dimensional Heisenberg Hamiltonian with symmetric biquadratic exchange and single-ion anisotropy to model the evolution of the NC phase above the CL-3 phase within a unit cell containing three independent spins.

The anharmonic CNC and NC-5 states predicted in this Letter cannot be approximated by the simple spirals assumed in earlier work. For example, the CNC state for $D/|J_1| = 0.2$ and $2\mu_B H/S|J_1| = 1$ is given by $Q = 0.856\pi$, $S_0 = 0.056S$, $C_1 = 1.155S$, $C_2 = -0.079S$, $C_3 = -0.170S$, $C_4 = 0.023S$, and $C_5 = 0.015S$. A simple spiral would have no anharmonic terms ($C_{l>1} = 0$). With decreasing field, the even harmonics of the CNC state decrease (they vanish as $H \to 0$) and the odd harmonics increase. The higher harmonics of the CNC phase can, in principle, be picked out by elastic neutron-scattering measurements.

Both Lummen *et al.* [23] and Terada *et al.* [24] have suggested that a magnetic field restores the symmetry of the triangular lattice that is broken by lattice distortions in zero field. In particular, Lummen *et al.* [23] argued that the anisotropy $D(H)$ decreases with field H. This would explain why magnetization measurements bypass the CL-5ii phase with $M = 0.6$: following the trajectory plotted in Fig. 2, the anisotropy would be reduced below about $0.28|J_1|$ in fields high enough to access the CL-5ii phase. However, excess ($\delta > 0$) or deficient ($\delta < 0$) oxygen in the nonstoichiometric compound $CuFeO_{2+\delta}$ may enhance the anisotropy D by introducing $L = 2$ Fe^{2+} or Cu^{2+} impurities. So it may be possible to enter the CL-5ii phase by using both field and oxygen nonstoichiometry to tune the position within the phase diagram.

Since the energy of the incommensurate CNC state was evaluated using a variational approach with six parameters whereas the energies of other states were obtained more precisely, the phase space of the CNC region may be *underestimated* compared to the phase space of the CL, SF, and NC-5 regions. On the other hand, interlayer interactions are expected to favor the CL states. Consequently, the NC-5 and SF regions in $CuFeO_2$ may be smaller than indicated by Fig. 2.

Along the trajectory of the solid curve in Fig. 2, the spin state passes through a complex series of transitions: CL-4 → CNC → NC-5i → CL-5i → NC-5ii → CL-3 → NC-5iii → SF → PM with critical fields H_{c1} through H_{c8} indicated on the right-hand side of Fig. 2. Most of these phase transitions have been observed in either pure, doped, or nonstoichiometric $CuFeO_2$.

For an Al doping of 1.2%, Kanetsuki *et al.* [9] described the predicted NC-5i phase above $H_{c2} \approx 12$ T: a phase with the same wave vector $\mathbf{Q} = 0.8\pi\mathbf{x}$ as the CL-5i phase but with M that increases linearly with field. For a Ga doping of 3.5%, Seki *et al.* [25] also reported the CNC → NC-5i transition at 12 T. Because the NC-5i phase has the same $\mathbf{Q}$ as the CL-5i phase but a similar field-dependent M as the CNC phase, it could easily have been mistaken for one or the other in pure $CuFeO_2$. Hysteresis at the first-order CNC → NC-5i transition [7–9] may also make it difficult to separate the NC-5i from the CNC and CL-5i states.

With either deficient or excess oxygen, Hasegawa *et al.* [13] observed transitions at $H_{c4} \approx 21$ and $H_{c5} \approx 23$ T, which may bracket the NC-5ii phase. In pure $CuFeO_2$, Lummen *et al.* [23] detected the CL-3 → NC-5iii transition at $H_{c6} \approx 32$ T and Quiron *et al.* [22] detected the NC-5iii → SF transition at $H_{c7} \approx 49$ T.

As seen in Fig. 2, the SF transition can be significantly reduced with doping. In a compound with 3.5% Ga, recent measurements [25] suggest that $D/|J_1| \approx 0.2$, corresponding to a SF transition field $H_{c7} \approx 30$ T. Because the chirality $\mathbf{C}$ of the SF state is perpendicular to $\mathbf{Q}$, it may be multiferroic with the same coupling mechanism predicted for manganites like $TbMnO_3$ [2].

Although the NC-5 states are chiral and possibly multiferroic, polarization measurements up to 43 T for a pure compound [26] and up to 14 T for a 3.5% Ga-doped compound [25] reported ferroelectric behavior only for the CNC phase between H_{c1} and H_{c2}. While the absence of ferroelectric behavior above H_{c2} might be caused by $\mathbf{Q}$ domains, a more likely explanation is that ferroelectric coupling is simply absent for the NC-5 states. Since both the CNC and NC-5 states break inversion symmetry, the absence of ferroelectric coupling for the NC-5 states would pose a significant challenge to theories of the coupling mechanism in multiferroic materials.

To summarize, the magnetic phase diagram of a geometrically frustrated TLA with exchange interactions up to third-nearest neighbors contains a remarkable diversity of magnetic phases, including five different CL phases, a SF phase, an incommensurate CNC phase with variable wave vector, and three different NC phases with 5-SL periodicity. Hopefully, future measurements on $CuFeO_2$ will be able to disentangle some of these closely related phases.

I would like to acknowledge helpful discussions with Dr. Feng Ye and Dr. Tsuyoshi Kimura. Research sponsored by the U.S. Department of Energy, Office of Basic Energy Sciences, Materials Sciences and Engineering Division.

[1] D. I. Khomskii, J. Magn. Magn. Mater. **306**, 1 (2006); S.-W. Cheong and M. Mostovoy, Nature Mater. **6**, 13 (2007).
[2] H. Katsura, N. Nagaosa, and A. V. Balatsky, Phys. Rev. Lett. **95**, 057205 (2005); M. Mostovoy, Phys. Rev. Lett. **96**, 067601 (2006).
[3] T. Nakajima, S. Mitsuda, S. Kanetsuki, K. Prokes, A. Podlesnyak, H. Kimura, and Y. Noda, J. Phys. Soc. Jpn. **76**, 043709 (2007); T. Nakajima, S. Mitsuda, S. Kanetsuki, K. Tanaka, K. Fujii, N. Terada, M. Soda, M. Matsuura, and K. Hirota, Phys. Rev. B **77**, 052401 (2008).
[4] S. Seki, Y. Onose, and Y. Tokura, Phys. Rev. Lett. **101**, 067204 (2008).
[5] C. Jia, S. Onoda, N. Nagaosa, and J. H. Han, Phys. Rev. B **74**, 224444 (2006).
[6] T. Arima, J. Phys. Soc. Jpn. **76**, 073702 (2007).
[7] S. Mitsuda, M. Mase, K. Prokes, H. Kitizawa, and H. A. Katori, J. Phys. Soc. Jpn. **69**, 3513 (2000).
[8] N. Terada, S. Mitsuda, K. Prokes, O. Suzuki, H. Kitazawa, and H. A. Katori, Phys. Rev. B **70**, 174412 (2004).
[9] S. Kanetsuki, S. Mitsuda, T. Nakajima, D. Anazawa, H. A. Katori, and K. Prokes, J. Phys. Condens. Matter **19**, 145244 (2007).
[10] R. S. Fishman and S. Okamoto, Phys. Rev. B **81**, 020402 (2010).
[11] R. S. Fishman, J. Appl. Phys. **103**, 07B109 (2008).
[12] J. T. Haraldsen, F. Ye, R. S. Fishman, J. A. Fernandez-Baca, Y. Yamaguchi, K. Kimura, and T. Kimura, Phys. Rev. B **82**, 020404 (2010); J. T. Haraldsen and R. S. Fishman, Phys. Rev. B **82**, 144441 (2010).
[13] M. Hasegawa, M. I. Batrashevich, T. R. Zhao, H. Takei, and T. Goto, Phys. Rev. B **63**, 184437 (2001).
[14] T. Takagi and M. Mekata, J. Phys. Soc. Jpn. **64**, 4609 (1995).
[15] M. Swanson, J. T. Haraldsen, and R. S. Fishman, Phys. Rev. B **79**, 184413 (2009); J. T. Haraldsen, M. Swanson, G. Alvarez, and R. S. Fishman, Phys. Rev. Lett. **102**, 237204 (2009).
[16] Because the conditions for global and local stability are different, R. S. Fishman and J. T. Haraldsen (unpublished) found that the boundary between the CL-4 subregions is slightly shifted from that given in Ref. [15].
[17] F. Ye, J. A. Fernandez-Baca, R. S. Fishman, Y. Ren, H. J. Kang, Y. Qiu, and T. Kimura, Phys. Rev. Lett. **99**, 157201 (2007); R. S. Fishman, F. Ye, J. A. Fernandez-Baca, J. T. Haraldsen, and T. Kimura, Phys. Rev. B **78**, 140407(R) (2008).
[18] M. E. Zhitomirsky and I. A. Zaliznyak, Phys. Rev. B **53**, 3428 (1996).
[19] The notation $m(n, l)$ is commonly used for a CL-m state with n spins up, $l = m - n$ spins down, and $M = (n - l)/m$. But that notation is not unique: both ↑↑↑↓↓ and ↑↑↓↑↓ states are denoted 5(3,2).
[20] Y. Ajiro, T. Asano, T. Takagi, M. Mekata, H. A. Katori, and T. Goto, Physica (Amsterdam) **201B**, 71 (1994).
[21] M. L. Plumer, Phys. Rev. B **76**, 144411 (2007); **78**, 094402 (2008).
[22] G. Quirion, M. L. Plumer, O. A. Petrenko, G. Balakrishnan, and C. Proust, Phys. Rev. B **80**, 064420 (2009).
[23] T. T. A. Lummen, C. Strohm, H. Rakoto, A. A. Nugroho, and P. H. M. van Loosdrecht, Phys. Rev. B **80**, 012406 (2009).
[24] N. Terada, Y. Tanaka, Y. Tabata, K. Katsumata, A. Kikkawa, and S. Mitsuda, J. Phys. Soc. Jpn. **75**, 113702 (2006).
[25] S. Seki, H. Murakawa, Y. Onose, and Y. Tokura, Phys. Rev. Lett. **103**, 237601 (2009).
[26] H. Mitamura, S. Mitsuda, S. Kanetsuki, H. A. Katori, T. Sakakibara, and K. Kindo, J. Phys. Soc. Jpn. **76**, 094709 (2007).